Further constraints on variation of the fine structure constant from alkali doublet QSO absorption lines*

M. T. Murphy[1][†], J. K. Webb[1], V. V. Flambaum[1], J. X. Prochaska[2] and A. M. Wolfe[3]

[1] *School of Physics, The University of New South Wales, UNSW Sydney NSW 2052, Australia*

[2] *The Observatories of the Carnegie Institute of Washington, 813 Santa Barbara St. Pasadena, CA 91101*

[3] *Department of Physics and Center for Astrophysics and Space Sciences, University of California, San Diego,*
 C-0424, La Jolla, CA 920923

arXiv:astro-ph/0012421v3 22 Jul 2001

ABSTRACT

Comparison of quasar absorption line spectra with laboratory spectra provides a precise probe for variability of the fine structure constant, α, over cosmological time-scales. We constrain variation in α in 21 Keck/HIRES Si IV absorption systems using the alkali doublet (AD) method in which changes in α are related to changes in the doublet spacing. The precision obtained with the AD method has been increased by a factor of 3: $\Delta\alpha/\alpha = (-0.5 \pm 1.3) \times 10^{-5}$. We also analyse potential systematic errors in this result. Finally, we compare the AD method with the many-multiplet method which has achieved an order of magnitude greater precision and we discuss the future of the AD method.

Key words: atomic data – line: profiles – techniques: spectroscopic – quasars: absorption lines – ultraviolet: general

1   INTRODUCTION

An experimental search for variation in the fine structure constant, $\alpha \equiv e^2/\hbar c$, is strongly motivated by many modern theories. In particular, theories attempting to unify gravitation with the other fundamental interactions, such as superstring theory, often require the existence of extra, 'compactified', spatial dimensions. The scale size of the extra dimensions is related to the values of the fundamental constants in our observable 4–dimensional subspace. Thus, evolution of these scale sizes with cosmology leads to time variation of the fundamental constants, such as α (e.g. Forgács & Horváth 1979; Marciano 1984; Barrow 1987; Damour & Polyakov 1994). Currently, it seems that there is no theoretical mechanism for keeping the extra dimensions constant in size (Li & Gott 1998) and so such theories naturally predict variation of α.

Quasar (QSO) absorption line studies provide a powerful probe of such variation. Savedoff (1956) first analysed

doublet separations seen in galaxy emission spectra to obtain constraints on variation of α. Absorption lines in intervening clouds along the line of sight to QSOs are substantially narrower than intrinsic emission lines and therefore provide a more precise probe of α. Bahcall, Sargent & Schmidt (1967) first used alkali doublet (AD) spacings of gas seen in absorption which seemed to be intrinsic to the QSO. They obtained the constraint $\Delta\alpha/\alpha \equiv (\alpha_z - \alpha_0)/\alpha_0 = (-2 \pm 5) \times 10^{-2}$ at a redshift $z \approx 1.95$. Here, α_z and α_0 are the values of α at the absorption redshift, z, and in the laboratory respectively. Since then, several authors (e.g. Cowie & Songaila 1995; Varshalovich, Panchuk & Ivanchik 1996) have applied the AD method to doublets of several species (e.g. C IV, Si II, Si IV, Mg II, Al III etc.) arising from intervening absorption clouds at significantly lower redshift than the background QSO.

The most recent and stringent constraint using the AD method was obtained by Varshalovich, Potekhin & Ivanchik (2000, hereafter VPI00) using the Si IV $\lambda 1393/1402$ doublet. A change in α will lead to a change in the doublet separation given by (VPI00, correcting a typographical error)

$$\Delta\alpha/\alpha = \frac{c_r}{2}\left[\frac{(\Delta\lambda/\lambda)_z}{(\Delta\lambda/\lambda)_0} - 1\right].\tag{1}$$

Here, $(\Delta\lambda/\lambda)_z$ and $(\Delta\lambda/\lambda)_0$ are the relative doublet separations in the absorption cloud (at redshift z) and in the

laboratory respectively and $c_r \approx 1$ is a constant taking into account higher order relativistic corrections. From 16 absorption systems (towards 6 QSOs) they obtained a mean $\Delta\alpha/\alpha = (-4.6 \pm 4.3) \times 10^{-5}$ using a line fitting method. The error quoted here is statistical only. VPI00 augment this with an additional systematic error term, $\pm 1.4 \times 10^{-5}$, due to uncertainties in the laboratory doublet separation, $(\Delta\lambda/\lambda)_0$, assumed in their analysis (see Table 1). This estimate of the potential systematic error seems optimistic considering that the error in the laboratory wavelength separation was previously quoted at $\delta(\Delta\lambda/\lambda)_0 \sim 1$ mÅ (Ivanchik, Potekhin & Varshalovich 1999). From equation 1, the corresponding systematic error in $\Delta\alpha/\alpha$ is

$$|\delta(\Delta\alpha/\alpha)| \approx -\frac{c_r}{2} \frac{\delta(\Delta\lambda/\lambda)_0}{(\Delta\lambda/\lambda)_0} \approx 5 \times 10^{-5} \qquad (2)$$

which is more consistent with the value reported by Ivanchik et al. (1999) ($\sim 8 \times 10^{-5}$) than by VPI00.

There are three ways in which the above constraints can be significantly improved without the need for a much larger sample:

(i) Improved spectral resolution: Many of the spectra used by VPI00 have FWHM ~ 20 kms^{-1} (e.g. Petitjean, Rauch & Carswell 1994; Varshalovich et al. 1996) while many absorption systems are known to contain Si IV lines with b-parameters (i.e. Doppler widths) ~ 5 kms^{-1} (e.g. Outram, Chaffee & Carswell 1999). FWHM ~ 7 kms^{-1} is now routinely used for QSO observations with, for example, the Keck/HIRES and the VLT/UVES. Therefore, such spectra offer the opportunity to significantly improve constraints on $\Delta\alpha/\alpha$.

(ii) Improved signal-to-noise ratio (SNR): Many of the spectra used by VPI00 have SNR ~ 15 per pixel. With the advent of 8–10 m telescopes, significantly greater SNR can be achieved (e.g. Prochaska & Wolfe 1996, 1997, 1999).

(iii) Improved laboratory wavelength measurements: Griesmann & Kling (2000) have increased the absolute precision of the laboratory wavelengths of Si IV $\lambda 1393$ and 1402 by more than two orders of magnitude. We compare the new values with those used by VPI00 (Kelly 1987; Morton 1991, 1992) in Table 1. Note that even our conservative estimate of the systematic error on $\Delta\alpha/\alpha$ in equation 2 is too small. The new measurements imply that the VPI00 result in equation 1 should be corrected by $\approx 11.3 \times 10^{-5}$ to $\Delta\alpha/\alpha \approx (7 \pm 4) \times 10^{-5}$. If the error in the difference between the doublet wavelengths is equal to the absolute uncertainty (i.e. 4×10^{-5} Å) then a precision limit of $\delta(\Delta\alpha/\alpha) \approx 0.2 \times 10^{-5}$ can now be reached. This should be true of Griesmann & Kling's measurement since statistical errors in the line positions dominated their error budget (Ulf Griesmann, private communication).

We apply the above improvements in the present work with the aim of increasing both the accuracy and precision of $\Delta\alpha/\alpha$ as measured using the Si IV AD method. The paper is organised as follows. Section 2 describes our observations, analysis methods and results. We investigate potential instrumental and astrophysical systematic effects in Section 3. We summarise our work in Section 4 and compare our results with others in the literature. We also compare the AD method with another method, the many-multiplet (MM)

method (Dzuba, Flambaum & Webb 1999a,b; Webb et al. 1999), which offers an order of magnitude greater precision.

2   DATA, ANALYSIS AND RESULTS

2.1   Keck/HIRES observations

All our QSO spectra were obtained at the Keck I 10 m telescope on Mauna Kea with the HIRES facility (Vogt et al. 1994) over several observing runs from 1994 to 1997. The QSOs were generally quite faint ($m_V \lesssim 19.0$) so several $\sim$1–2 hour exposures were co-added for each object. Most of the data were reduced using the HIRES data reduction package written by T. Barlow, MAKEE. This package converts the two-dimensional echelle images to fully reduced, one-dimensional, wavelength–calibrated spectra.

Thorium–Argon (ThAr) calibration spectra were taken before and after the QSO exposures and co-added to provide a calibration spectrum. ThAr lines were selected and centroided to provide a wavelength solution. Some of the spectra were reduced when MAKEE had no wavelength calibration facility. In these cases, wavelength calibration was carried out using IRAF[‡] routines. Spectra not reduced in MAKEE were fully reduced within IRAF. 1σ error arrays were generated assuming Poisson counting statistics. We fit continua to regions of each spectrum containing either or both of the Si IV doublet transitions by fitting Legendre polynomials to ~ 500 kms^{-1} sections. Full details of the reduction procedures can be found in Prochaska & Wolfe (1996, 1997, 1999). Outram et al. (1999) have also kindly contributed their spectrum of Q1759+75 taken in July 1997.

Our sample comprises 21 Si IV absorption systems (towards 8 QSOs) over a redshift range $z = 2$–3 (mean $z = 2.6$). The SNR per pixel ranges from 15–40 with most spectra having SNR ~ 30 and FWHM $\lesssim 7.5$ kms^{-1} ($R = 34000$). We provide an example absorption system in Fig. 1.

2.2   Analysis

Although equation 1 is a simple approach to the specific case of an alkali doublet, a more general approach is to write down the energy equation for an individual transition, within any multiplet and for any species. Dzuba et al. (1999a,b) and Webb et al. (1999) suggested the convenient formulation

$$\omega_z = \omega_0 + q_1 x + q_2 y, \qquad (3)$$

where ω_z is the wavenumber in the rest-frame of the cloud, at redshift z, in which α_z/α_0 may not equal unity. ω_0 is the wavenumber as measured in the laboratory and x and y contain the information about $\Delta\alpha/\alpha$: $x \equiv \left(\frac{\alpha_z}{\alpha_0}\right)^2 - 1$, $y \equiv \left(\frac{\alpha_z}{\alpha_0}\right)^4 - 1$. The q_1 and q_2 coefficients represent the relativistic corrections to the energy for a particular transition. The q_1 coefficients are typically an order of magnitude larger than the q_2 coefficients and so it is the relative magnitudes

Table 1. Atomic data for the Si IV λ1393 and 1402 lines. We give the ground and excited state configurations and compare the new laboratory wavelength measurements with those used by VPI00. We also give the oscillator strengths, f, used in our profile fitting algorithm and the relativistic coefficients q_1 and q_2 used in equation 3.

Transition	Ground	Upper state	Old $\lambda_0/\text{Å}$ [a]	New $\lambda_0/\text{Å}$ [b]	New ω_0/cm^{-1} [b]	f [a]	q_1/cm^{-1} [c]	q_2/cm^{-1} [c]
Si IV λ1393	$2p^63s\ ^2\text{S}_{1/2}$	$2p^63p\ ^2\text{P}_{3/2}$	1393.755(6)	1393.76018(4)	71748.355(2)	0.5140	766	48
Si IV λ1402		$2p^63p\ ^2\text{P}_{1/2}$	1402.770(6)	1402.77291(4)	71287.376(2)	0.2553	362	-8

[a]Martin & Zalubas (1983) and Kelly (1987); [b]Griesmann & Kling (2000); [c]Dzuba, Flambaum & Webb (1999b)
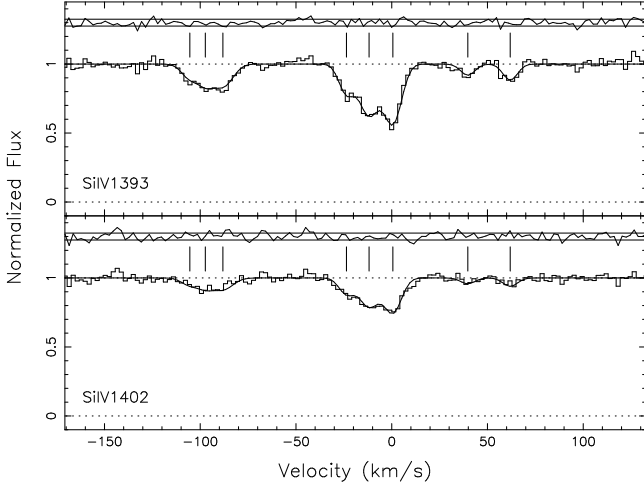

Figure 1. Si IV absorption system at $z = 2.530$ towards the QSO 2348-14. The data have been normalized by a fit to the continuum and plotted as a histogram. Our Voigt profile fit (solid curve) and the residuals (i.e. [data] − [fit]), normalized to the 1σ errors (horizontal solid lines), are also shown. The tick–marks above the continuum indicate individual velocity components.

of q_1 for different transitions that characterizes our ability to constrain $\Delta\alpha/\alpha$. This equation forms the basis of the MM method (see Section 4.1). In the case of a single alkali doublet and $\Delta\alpha/\alpha \ll 1$, equation 3 reduces to equation 1 with

$$c_r \approx \frac{\delta q_1 + \delta q_2}{\delta q_1 + 2\delta q_2} \qquad (4)$$

where δq_1 and δq_2 are the differences between the q_1 and q_2 coefficients for the doublet transitions. The values for q_1 and q_2 for Si IV λ1393 and 1402 have been calculated by Dzuba et al. (1999b) and are shown in Table 1. For the Si IV doublet, $c_r \approx 0.9$ as used by VPI00.

Our technique is based on a simultaneous χ^2 minimization analysis of multiple component Voigt profile fits to the Si IV absorption features in the QSO spectra. Consider a QSO spectrum containing a single velocity component of a specific transition. Three parameters describe the Voigt profile fit to such a component: the column density N, the Doppler width or b-parameter and the redshift z of the absorbing gas cloud. For the present case, we add another free parameter to the fit: $\Delta\alpha/\alpha$.

We have used the program VPFIT[§] (Webb 1987) to fit absorption profiles to the spectra. We have modified VPFIT to include $\Delta\alpha/\alpha$ as a free parameter. Parameter errors can be calculated from the diagonal terms of the final parameter covariance matrix (Fisher 1958). The reliability of these errors has been confirmed using Monte Carlo simulations of a variety of different combinations of transitions and velocity structures.

VPFIT imposes a cut-off point in parameter space such that very weak velocity components are removed from the fit when they no longer significantly affect the value of χ^2. Conceivably, dropping even very weak components could affect our determination of $\Delta\alpha/\alpha$. Therefore, in such cases we observed the trend in the values of $(\Delta\alpha/\alpha)_i$ at each iteration i of the minimization routine to see if this trend was significantly altered due to line dropping. If components were dropped during a fit then we also re-ran the VPFIT algorithm, keeping the dropped components by fixing their column density at the value just before they were dropped from the original fit. No cases were found where the values of $\Delta\alpha/\alpha$ from the different runs differed significantly.

We impose several consistency checks before we accept a value of $\Delta\alpha/\alpha$. Firstly, the value of χ^2 per degree of freedom must be $\sim$1. Secondly, we calculated $\Delta\alpha/\alpha$ for each absorption system using a range of different first-guess values for $\Delta\alpha/\alpha$ to ensure that the VPFIT algorithm was finding global minima in the χ^2 parameter space.

2.3 Results

We present our results in Table 2. We show our values of $\Delta\alpha/\alpha$ for each absorption cloud together with the 1σ error bars derived from the VPFIT algorithm. To illustrate the distribution of $\Delta\alpha/\alpha$ over cosmological time, we plot these results in Fig. 2 as a function of fractional look-back time to the cloud and the absorption cloud redshift, z. The weighted mean of the sample is $\Delta\alpha/\alpha = (-0.5 \pm 1.3) \times 10^{-5}$. Our results show a 3.3-fold increase in precision over the VPI00 result. The reduced χ^2 about the weighted mean value is 0.95, which gives no evidence to suggest that we may have incorrectly estimated the individual 1σ errors on $\Delta\alpha/\alpha$. We checked that the distribution of $\Delta\alpha/\alpha$ values shows no gross deviation from a Gaussian distribution (although with only 21 data points this is not a rigorous check). We also note that the unweighted ($\Delta\alpha/\alpha = (-0.12 \pm 1.4) \times 10^{-5}$) and

[§] See http://www.ast.cam.ac.uk/~rfc/vpfit.html for details about obtaining VPFIT.

Table 2. The raw results from the χ^2 minimization procedure. For each QSO sight line we identify the QSO emission redshift, $z_{\rm em}$, the absorption cloud redshift, $z_{\rm abs}$ and the value of $\Delta\alpha/\alpha$ for each absorption cloud.

Object	$z_{\rm em}$	$z_{\rm abs}$	$\Delta\alpha/\alpha/10^{-5}$
0100+13	2.68	2.299	-3.05 ± 7.30
		2.309	8.96 ± 10.39
0149+33	2.43	2.065	-4.47 ± 16.81
		2.140	-12.93 ± 12.69
		2.204	-5.89 ± 6.68
0201+36	2.49	2.457	-4.50 ± 3.57
0347−38	3.24	2.810	3.04 ± 7.43
		2.899	-10.90 ± 10.87
		3.025	-4.05 ± 6.78
1759+75	3.05	2.624^a	-5.98 ± 2.98
		2.849^a	2.56 ± 3.29
		2.849	2.74 ± 3.88
		2.911	6.00 ± 9.89
		2.911^a	0.65 ± 4.75
2206−20	2.56	2.014	-3.84 ± 6.59
		2.128	-3.48 ± 7.41
2231−00	3.02	2.641	0.20 ± 10.65
		2.986	4.23 ± 17.74
2348−14	2.94	2.279	10.38 ± 6.05
		2.530	3.76 ± 6.53
		2.775	14.04 ± 7.10

^{a}These absorbers contributed by Outram, Chaffee & Carswell (1999)

weighted means are consistent with each other, again suggesting no substantial deviation from Gaussianity.

3 POSSIBLE SYSTEMATIC ERRORS

Although our result is statistically insignificant, the precision obtained is approaching the level at which systematic errors begin to become important. We have already discussed how the VPI00 result was severely effected by errors in the laboratory wavelengths of Si IV λ1393 and 1402. We must therefore examine possible systematic errors in our results. We have considered a range of instrumental and astrophysical systematic errors particular to the MM method in Murphy et al. (2001b, hereafter M01b). Below we discuss some of these in the context of the Si IV AD method.

3.1 Wavelength mis-calibration

The wavelength calibration of the QSO CCD images is done by comparison with Thorium–Argon (ThAr) lamp exposures taken before and after the QSO frames. We consider errors in the laboratory wavelengths of the selected ThAr lines to be negligible as their relative values are known to a similar precision as our values of ω_0 (Palmer & Engleman Jr. 1983). However, ThAr line mis-identifications may lead to serious mis-calibration of the wavelength scale over large wavelength regions. Such mis-identifications can also be applied to the rest of the spectra taken over the same series of observations (i.e. applied to the spectra of many QSOs). Thus, *a priori*, we cannot rule out the possibility that the wavelength scale has been set improperly in this process and that a systematic
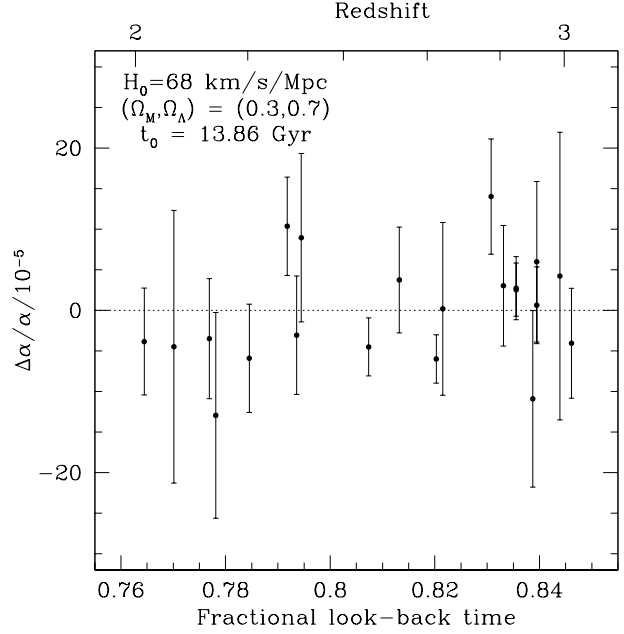

Figure 2. Our values of $\Delta\alpha/\alpha$ for each absorption cloud plotted against fractional look-back time (using the specified cosmological model) and redshift. The weighted mean of the sample is $\Delta\alpha/\alpha = (-0.5 \pm 1.3) \times 10^{-5}$.

shift in α has not been mimicked. Such a potential effect needs careful investigation.

We designed a direct test for wavelength mis-calibration in M01b: we treated the ThAr emission lines in the calibration spectra with the same analysis used to derive $\Delta\alpha/\alpha$ from the QSO absorption lines in the object spectra. We have applied this method to the ThAr spectra corresponding to the absorption systems in our sample. For each absorption system we derive values of $(\Delta\alpha/\alpha)_{\rm ThAr}$ from corresponding sections of ThAr spectra using the same analysis technique outlined in Section 2.2 with the following modifications:

(i) We fit Gaussian profiles to the ThAr emission lines (instead of Voigt profiles which were fitted to the QSO absorption lines).

(ii) We use the literature wavenumbers of the selected ThAr lines (Palmer & Engleman Jr. 1983) for ω_0 in equation 3. However, we use the q_1 and q_2 coefficients of the Si IV lines. For example, if we select a ThAr line lying in the same region of the spectrum as the Si IV λ1393 line of interest, then we assign the q_1 and q_2 coefficients for Si IV λ1393 to that ThAr line.

(iii) In M01b we noted that the χ^2 for a fit to a set of ThAr lines was $\gg 1$ (in the present case, this 'set' contains two ThAr lines lying in the same spectral regions as the corresponding Si IV lines). This was attributed to weak blends in the selected ThAr lines. This was also observed in the present analysis. In this case, we cannot use the 1σ error on $(\Delta\alpha/\alpha)_{\rm ThAr}$ generated by VPFIT. Therefore, we select several different sets of ThAr lines and find $(\Delta\alpha/\alpha)_{\rm ThAr}$ for each set. The error in $(\Delta\alpha/\alpha)_{\rm ThAr}$ is then taken as the error in the mean value for the different sets.

Our results are shown in Fig. 3 where we compare them with the results from the QSO data. It is clear that the QSO
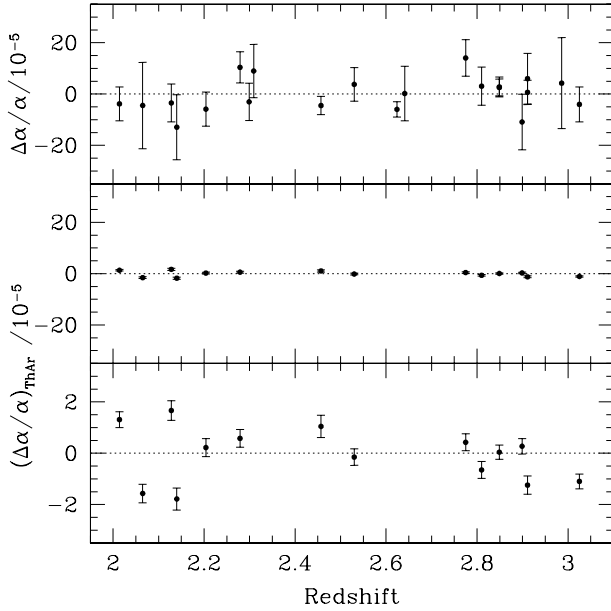
Figure 3. Comparison of QSO and ThAr results. The top panel shows the QSO results and the middle panel shows the ThAr data on the same scale. The weighted mean is $(-6 \pm 9) \times 10^{-7}$. The lower panel is an expanded view of the ThAr results. Note that some ThAr data was not available. Clearly, this does not affect our conclusions.

results have not been significantly affected in any systematic way. The weighted mean value of $(\Delta\alpha/\alpha)_{\text{ThAr}} = (-6 \pm 9) \times 10^{-7}$. The scatter in the data is larger than what we expect on the basis of the individual error bars. This could be due to either real (low level) mis-calibrations or to the line blending discussed above.

The results in Fig. 3 are also relevant for possible variations in instrumental profile (IP) asymmetry along and across echelle orders. Valenti, Butler & Marcy (1995) have determined the HIRES IP for several positions along a single order and they find that the IP is indeed asymmetric and that the asymmetry varies slightly along the echelle order. However, Fig. 3 shows that any asymmetry variations have not systematically affected our determination of $\Delta\alpha/\alpha$.

3.2 Systematic line blending with unknown species

There may have been weak, interloping, unresolved lines which, if the interloping species were in the same absorption cloud, could have produced a shift in the fitted line wavelengths of all velocity components of one or both Si IV transitions. We distinguish between *random* blends and *systematic* blends. *Random* blends may occur if many absorption clouds at different redshifts intersect the line of sight to a single QSO. A *systematic* blend will occur when two species are in the same cloud and have absorption lines with similar rest-wavelengths. Such an effect could mimic a systematic shift in α.

We have searched atomic line databases (Moore 1971; the Vienna Atomic Line Database (VALD) – Piskunov et al. 1995 and Kupka et al. 1999) for transitions of any species

which may blend with Si IV $\lambda 1393$ or 1402. The search was restricted to transitions from the ground state with rest wavelengths λ such that $|\lambda - \lambda_0| \leq 0.2\,\text{Å}$. This is a conservative upper limit adopted from simulations of typical blends in M01b. We did not identify any potential blends with Si IV $\lambda 1402$ satisfying this criteria. For Si IV $\lambda 1393$ we found one potential interloper: Be I $\lambda 1393$ at $\lambda = 1393.804\,\text{Å}$ (VALD). This transition has an oscillator strength of $f = 2.080 \times 10^{-3}$. The Be I $\lambda 2349$ transition is nearly three orders of magnitude stronger than this ($f = 1.698$) and, to our knowledge, has never been detected in QSO absorption spectra. This safely rules out Be I $\lambda 1393$ as a candidate interloper.

In summary, we have found no known atomic transitions which may blend with either of the Si IV doublet lines. We have not considered molecular transitions as potential interlopers but consider this possibility to be unlikely (see M01b for discussion).

3.3 Differential isotopic saturation

Si has three naturally occurring isotopes, ^{28}Si, ^{29}Si and ^{30}Si, with terrestrial abundances in the ratio $92.23 : 4.68 : 3.09$ (Rosman & Taylor 1998). Thus, each absorption line will be a composite of absorption lines from all three isotopes. We are not aware of any experimental determinations of the spectral separations between the isotopic components. Thus, the values of ω_0 in Table 1 (Griesmann & Kling 2000) are *composite* wavenumbers only. These wavenumbers will only strictly be applicable in the optically thin regime (linear part of the curve of growth). As the column density increases, the strongest isotopic component begins to saturate and the line centroid will shift according to the natural abundances (cf. Section 3.4) of the other isotopes.

Estimates of the isotopic separations for the Si IV doublet have been made by W. R. Johnson (private communication) and these are summarised in Table 3. From these separations we have estimated the absolute isotopic wavenumbers (ω_0 in Table 3) such that the abundance-weighted mean of the isotopic wavenumbers equals the composite values in Table 1. The error in these results is $\lesssim 10\%$ and comes from errors in the isotopic separations.

If we consider a Si IV doublet with a single velocity component then, as the $\lambda 1393$ line begins to saturate, the line centroid will shift bluewards. The effective doublet separation will continue to increase but this increase will eventually slow and reverse as the $\lambda 1402$ transition begins to saturate. It is clear that this is a potentially important systematic effect for the Si IV doublet. Therefore, we have used the values of ω_0 in Table 3 to re-calculate $\Delta\alpha/\alpha$ for our sample of Si IV absorbers. Only 5 systems clearly contain saturated components and $\Delta\alpha/\alpha$ in these systems displays the expected behaviour: $\Delta\alpha/\alpha$ becomes more negative when the isotopic structures are included. Overall, the weighted mean for our sample becomes $\Delta\alpha/\alpha = (-0.8 \pm 1.3) \times 10^{-5}$.

3.4 Isotopic abundance variation

Timmes & Clayton (1996) suggest that the abundance of ^{29}Si and ^{30}Si should decrease with decreasing metallicity. In general, damped Lyman-α systems (DLAs), which some of

Table 3. The isotopic structures of Si IV $\lambda 1393$ and 1402 calculated by W. R. Johnson (private communication). We show the total isotopic separation, $\Delta\omega_0^{\mathrm{tot}}$, and the contribution from the specific ($\Delta\omega_0^{\mathrm{spec}}$) and volume ($\Delta\omega_0^{\mathrm{vol}}$) isotopic shifts. The final wavenumber, ω_0, is such that the abundance-weighted mean equals the corresponding composite value (see Table 1). The last column shows the relative abundance of each isotope (Rosman & Taylor 1998).

Transition	m/amu	$\Delta\omega_0^{\mathrm{tot}}/\mathrm{cm}^{-1}$	$\Delta\omega_0^{\mathrm{spec}}/\mathrm{cm}^{-1}$	$\Delta\omega_0^{\mathrm{vol}}/10^{-3}\,\mathrm{cm}^{-1}$	$\omega_0/\mathrm{cm}^{-1}$	$\lambda_0/\mathrm{\AA}$	%
Si IV $\lambda 1393$	28	—	—	—	71748.344	1393.76039	92.23
	29	0.1044	0.0585	—	71748.478	1393.75779	4.68
	30	0.2017	0.1130	4.413	71748.545	1393.75649	3.09
Si IV $\lambda 1402$	28	—	—	—	71287.365	1402.77313	92.23
	29	0.1042	0.0583	—	71287.499	1402.77049	4.68
	30	0.2013	0.1126	4.418	71287.566	1402.76917	3.09

our Si IV doublets are associated with, are thought to have metallicities $\lesssim -1$ at high redshift (e.g. Prochaska & Wolfe 2000). If the isotopic abundances of Si at redshifts $z = 2$–3 differ substantially from their terrestrial values then this may mimic a shift in α.

The dominant component of the isotopic shift is the mass shift: $\Delta\omega \propto \omega/m^2$ for m the atomic mass. Thus, for a single ion, the mass shift is degenerate with the redshift parameter fitted to the velocity components of an absorption system. That is, it will have no affect on our values of $\Delta\alpha/\alpha$. The specific isotopic shifts for the Si IV doublet have been calculated by W. R. Johnson (private communication) and are given in Table 3. We also show the volume isotopic shift for ^{30}Si IV as calculated by V. A. Dzuba (private communication) and these are clearly negligibly small. The specific shift is not degenerate with redshift but only at a negligible level. Thus, even if the isotopic ratios of ^{29}Si and ^{30}Si are much smaller in our Si IV absorbers, this will have a negligible affect on $\Delta\alpha/\alpha$.

3.5 Hyperfine structure effects

Hyperfine splitting can lead to saturation effects similar to the isotopic saturation effects discussed in Section 3.3. The transitions of the ^{29}Si isotope will experience hyperfine splitting since the neutron number is odd. As with the isotopic structure, the magnitude of hyperfine splitting has not been measured. However, V. A. Dzuba (private communication) has estimated the splitting and finds it to be a factor of ~ 2 times smaller than the isotopic splitting. This may also be estimated by comparison with the hyperfine structure of ^{25}Mg since the Si IV and Mg II doublets have similar ground and excited state wavefunctions and the magnetic moments of Mg and Si are similar. Drullinger, Wineland & Bergquist (1980) have measured the hyperfine splitting of the ^{25}Mg II $\lambda 2796$ transition: the hyperfine splitting is ~ 2 times smaller than the isotopic separations. It is therefore clear that saturation effects will be negligible.

3.6 Atmospheric dispersion effects

As discussed in M01a, 5 of our absorption systems were observed without the use of an image rotator (i.e. they were observed before August 1996 when a rotator was installed on HIRES). The QSO light is dispersed across the spectrograph slit by the atmosphere and, if the slit is not maintained perpendicular to the horizon by an image rotator, light of different wavelengths will enter the spectrograph at slightly different angles. In M01b we discussed two effects resulting from this: (i) a bulk stretching of the spectra relative to the ThAr calibration frames and (ii) a distortion of the PSF due to truncation of the dispersed seeing disc on either side of the slit jaws. We do not consider (ii) any further since the effect on $\Delta\alpha/\alpha$ found in M01b was small and since the distortion should be very similar at both Si IV doublet wavelengths. We consider effect (i) below.

The optical design of HIRES at the time at which our affected data was taken was such that $\theta = \xi$ for θ the angle of the slit to the vertical and ξ the zenith angle of the object (Tom Bida, Steve Vogt, personal communications). Consider two wavelengths, λ_1 and λ_2 ($\lambda_2 > \lambda_1$), falling across the spectrograph slit. If we were to measure the spectral separation between these two wavelengths on the CCD, $\Delta\lambda'$, we would find that

$$\Delta\lambda' \approx \lambda_2 - \lambda_1 + \frac{a\Delta\psi\sin\theta}{\delta}\,, \tag{5}$$

where a is the CCD pixel size in Ångstroms, δ is the projected slit width in arc seconds per pixel (for HIRES, $\delta = 0\rlap{.}''287$ per pixel) and $\Delta\psi$ is the angular separation (in arc seconds) of λ_1 and λ_2 at the slit. $\Delta\psi$ is a function of the atmospheric conditions along the line of sight to the object and can be approximated using the refractive index of air at the observer and the zenith distance of the object (e.g. Filippenko 1982). Note that equation 5 is only valid if the seeing and tracking error are zero. These two effects will reduce the measured $\Delta\lambda'$.

For the Si IV doublet, a typical value for $\Delta\psi$ is only $\approx 0\rlap{.}''007$ (using atmospheric conditions typical of Mauna Kea, an absorption redshift $z = 2.6$ and $\psi = 30^\circ$, which is typical of our sample, see M01b). This implies $\Delta\lambda' - (\lambda_2 - \lambda_1) \approx 3.7 \times 10^{-4}$ Å with $a = 0.03$ Å per pixel and will mimic a shift in α, $\Delta\alpha/\alpha \approx +0.66 \times 10^{-5}$. The sign of this correction is such that removing the stretching implied by equation 5 from our data will result in a more negative $\Delta\alpha/\alpha$. The correction is substantial for an individual system so we have applied it to the 5 affected systems to obtain an upper limit on the overall affect on $\Delta\alpha/\alpha$. Our weighted mean value of $\Delta\alpha/\alpha$ for the entire sample becomes $(-0.6 \pm 1.3) \times 10^{-5}$.

4 DISCUSSION

4.1   Comparison with other results

We have increased the precision of $\Delta\alpha/\alpha$ as measured with the AD method by at least a factor of 3.3 over that of VPI00. The increase in precision (and accuracy) is due to improved data quality (higher spectral resolution and SNR) and greatly improved laboratory wavelength measurements (Griesmann & Kling 2000).

Despite this increase in precision, the MM method can provide a further increase of up to an order of magnitude with similar quality data. The MM method was first proposed by Dzuba, Flambaum & Webb (1999a,b) and Webb et al. (1999) (see also Dzuba et al. 2001). It is based on equation 3 and the use of many transitions, from many different multiplets in different ions. The q_1 coefficients of transitions in heavy ($m \sim 50$) ions are typically an order of magnitude larger than those for light ions ($m \sim 25$). Depending on the nature of the ground and excited state wavefunctions, the q_1 coefficients for some transitions may also be of opposite sign, even for transitions of the same ion. Therefore, the MM method has the following advantages over the AD method:

- The MM method allows us to probe an effect $\sim$10 times larger since we can compare total relativistic corrections (not just the spin orbit coupling probed by the AD method).
- In principle, all transitions appearing in the QSO spectra may be used and so the number of constraints on $\Delta\alpha/\alpha$ is increased.
- In practice, having a larger number of transitions leads to much better constraints on the velocity structure of the absorbing clouds.
- Comparison of transitions with positive and negative q_1 coefficients minimizes the systematic effects in Section 3.

Webb et al. (1999) demonstrated the MM method and found tentative evidence for a smaller α at redshifts $z \sim 1$: $\Delta\alpha/\alpha = (-1.09 \pm -0.36) \times 10^{-5}$. We have extended that work in M01a and Webb et al. 2001, analysing 21 high redshift DLAs and re-analysing 28 lower redshift Mg/Fe systems from the Webb et al. (1999) data set. We confirmed the Webb et al. result and found similar results for the DLAs in Murphy et al. (2001a) and Webb et al. (2001). For the entire sample ($0.5 < z < 3.5$), $\Delta\alpha/\alpha = (-0.72 \pm 0.18) \times 10^{-5}$. We analysed potential systematic errors in M01b and found that atmospheric dispersion effects and isotopic abundance variation may have led us to find a $\Delta\alpha/\alpha$ that was too positive (i.e. once these two effects are removed from our data, we find a more negative $\Delta\alpha/\alpha$). The results of M01a and M01b indicate possible variation in α. Even if these results are considered to be an upper limit on $\Delta\alpha/\alpha$, they are by far the most restrictive limits at high redshift. Our present result of $\Delta\alpha/\alpha = (-0.5 \pm 1.3) \times 10^{-5}$ is consistent with these results. We review constraints on $\Delta\alpha/\alpha$ at other redshifts in M01a.

4.2   The future for the Si IV AD method

If the AD method were to be used to reach a similar precision as reached in M01a, a SNR $\gtrsim 200$ in $\sim$50 systems would be required. In Section 3 we found that systematic errors important for the AD method can correspond to $|\Delta\alpha/\alpha| \sim 0.3 \times 10^{-5}$ which is of similar magnitude to the effect of systematic errors in the MM method (M01b).

Therefore, once these systematic errors are understood and can be reliably removed from QSO absorption data, the MM method is clearly the preferred method for probing $\Delta\alpha/\alpha$ at high redshift.

Despite this, a modest increase in precision could easily be achieved with our present data if the C IV $\lambda1548/1550$ doublet laboratory wavelengths were known to high enough precision. Griesmann & Kling (2000) have increased the laboratory precision by an order of magnitude but the statistical uncertainty in the wavelengths is still $\gtrsim 0.04\,\mathrm{cm}^{-1}$. If the laboratory precision can be increased by another order of magnitude, the Si IV and C IV doublet can be analysed simultaneously to obtain tighter constraints on $\Delta\alpha/\alpha$ (i.e. the MM method could be used).

REFERENCES

Bahcall J. N., Sargent W. L. W., Schmidt M., 1967, ApJ, 149, L11
Barrow J. D., 1987, Phys. Rev. D, 35, 1805
Cowie L. L., Songaila A., 1995, ApJ, 453, 596
Damour T., Polyakov A. M., 1994, Nucl. Phys. B, 423, 532
Drullinger R. E., Wineland D. J., Bergquist J. C., 1980, Appl. Phys., 22, 365
Dzuba V. A., Flambaum V. V., Webb J. K., 1999a, Phys. Rev. Lett., 82, 888
Dzuba V. A., Flambaum V. V., Webb J. K., 1999b, Phys. Rev. A., 59, 230
Dzuba V. A., Flambaum V. V., Murphy M. T., Webb J. K., 2001, Phys. Rev. A, 63, 042509
Filippenko A. V., 1982, PASP, 94, 715
Fisher R. A., 1958, Statistical methods for research workers. Harper, New York, USA
Forgács P., Horváth Z., 1979, General Relativity and Gravitation, 10, 931
Griesmann U., Kling R., 2000, ApJ, 526, L113
Ivanchik A. V., Potekhin A. Y., Varshalovich D. A., 1999, A&A, 343, 439
Kelly R. L., 1987, J. Phys. Chem. Ref. Data NBS, 16, Suppl. 1
Kupka F., Piskunov N. E., Ryabchikova T. A., Stempels H. C., Weiss W. W., 1999, A&AS, 138, 119
Li L. -X., Gott J. R. III, 1998, Phys. Rev. D, 58, 103513
Marciano W. J., 1984, Phys. Rev. Lett., 52, 489
Martin W. C., Zalubas R., 1987, J. Phys. Chem. Ref. Data, 12, 323
Moore C. E., 1971, Atomic Energy Levels As Derived From Analyses of Optical Spectra, Natl. Stand. Rel. Data Ser., Natl.

Bur. Stand. (U.S.A.), Vol 1 and 2, U.S. Govt. Print Office, Washington, D.C., U.S.A.

Morton D. C., 1991, ApJS, 77, 119

Morton D. C., 1992, ApJS, 81, 883

Murphy M. T., Webb J. K., Flambaum V. V., Dzuba V. A., Churchill C. W., Prochaska J. X., Barrow J. D., Wolfe A. M., 2001a, MNRAS, accepted (M01a) (astro-ph/0012419)

Murphy M. T., Webb J. K., Flambaum V. V., Churchill C. W., Prochaska J. X., 2001b, MNRAS, accepted (M01b) (astro-ph/0012420)

Outram P. J., Chaffee F. H., Carswell R. F., 1999, MNRAS, 310, 289

Palmer B. A., Engleman R. Jr., 1983, Atlas of the Thorium Spectrum, Los Alamos National Laboratory, Los Alamos, New Mexico

Petitjean P., Rauch M., Carswell R. F., 1994, A&A, 291, 29

Pickering J. C., Thorne A. P., Webb J. K., 1998, MNRAS, 300, 131

Piskunov N. E., Kupka F., Ryabchikova T. A., Weiss W. W., Jeffery C. S., 1995, A&AS, 112, 525

Prochaska J. X., Wolfe A. M., 1996, ApJ, 470, 403

Prochaska J. X., Wolfe A. M., 1997, ApJ, 474, 140

Prochaska J. X., Wolfe A. M., 1999, ApJS, 121, 369

Prochaska J. X., Wolfe A. M., 2000, ApJ, 533, L5

Rosman K. J. R., Taylor P. D. P., 1998, Pure and Applied Chemistry, 70, 217

Savedoff M. P., 1956, Nat, 178, 689

Timmes F. X., Clayton D. D., 1996, ApJ, 472, 723

Valenti J. A., Butler R. P., Marcy G. W., 1995, PASP, 107, 966

Varshalovich D. A., Panchuk V. E., Ivanchik A. V., 1996, Astron. Lett., 22, 6

Varshalovich D. A., Potekhin A. Y., Ivanchik A. V., 2000, in Dunford R. W., Gemmel D. S., Kanter E. P., Kraessig B., Southworth S. H., Young L., eds., AIP Conf. Proc. 506, X-ray and Inner-Shell Processes. Argonne National Laboratory, Argonne, Illinois, p. 503 (VPI00)

Vogt S. S. et al., 1994, in Crawford D. L., Craine E. R., eds., Instrumentation in Astronomy VIII, SPIE, 2198, 362

Webb J. K., 1987, Ph.D. thesis, Cambridge University

Webb J. K., Flambaum V. V., Churchill C. W., Drinkwater M. J., Barrow J. D., 1999, Phys. Rev. Lett., 82, 884

Webb J. K., Murphy M. T., Flambaum V. V., Dzuba V. A., Barrow J. D., Churchill C. W., Prochaska J. X., Wolfe A. M., 2001, Phys. Rev. Lett., accepted (astro-ph/0012539)